COLUMBIA | SIPA
Center for Environmental Economics and Policy

CEEP Working Paper Series
Working Paper Number 37

January 2026

Environmental Impacts of China's Overseas Development Projects

Xinming Du and Douglas Almond

https://ceep.columbia.edu/sites/default/files/content/papers/n37.pdf

Environmental Impacts of China's Overseas Development Projects*

Xinming Du† Douglas Almond‡

January 2026

Abstract

While the economic and social benefits of foreign aid and development finance receipt are well-established, relatively little is known about the environmental impacts in recipient countries. China has undertaken overseas investment projects on a massive scale across more than 140 countries. This paper quantifies their impacts on key ecological outcomes: deforestation, land use, air pollution, and biodiversity. Using 6,303 geocoded Chinese finance projects from 2000-2023 combined with satellite and biodiversity data, we find that project implementation leads to an immediate and persistent decline in surrounding vegetation by 0.3%, equivalent to an average annual loss of 4,755 km^2 of vegetated land worldwide. Air quality also deteriorates, with aerosol optical depth rising 0.9%. Biodiversity losses are concentrated among higher trophic groups: bird species richness declines by 1.6% and mammalian richness by 0.1%. Translating vegetation loss into reduced carbon sink capacity implies annual emissions of 52-174 million tons of CO_2e, corresponding to annual global welfare losses of $2.6-$33.1 billion.

JEL Classifications: Q56, F35, Q23, O13

Keywords: Overseas investment, land use, ecosystem disruption, deforestation, air pollution

*We thank Lucas Davis and Andreas Madestam for valuable comments and suggestions.

†Department of Economics, National University of Singapore. Email: xdu@nus.edu.sg

‡School of International and Public Affairs & Department of Economics, Columbia University & NBER. Email: da2152@columbia.edu

1 Introduction

Satellite-based studies document large global forest losses since 2000, particularly in tropical regions (Hansen et al., 2013). A large portion of this loss is linked to permanent land conversion associated with infrastructure expansion, agriculture, and industrial activity (Curtis et al., 2018). Official assessments underscore the massive scale of land-use changes: the FAO estimates that around 420 million hectares of forest were lost globally between 1990 and 2020, with deforestation continuing at 10 million hectares per year in the late 2010s (Food and Agriculture Organization of the United Nations, 2020). Land use change and deforestation are also estimated to contribute 10-15% of global anthropogenic greenhouse gas emissions, highlighting that development-driven vegetation loss is a quantitatively important channel of environmental externalities (Intergovernmental Panel on Climate Change, ed, 2021).

These ecological shifts are not evenly distributed but tend to be most severe in settings with weak environmental enforcement and insecure property rights. Where monitoring capacity is limited and penalties for land clearing are weakly enforced, large-scale projects can generate extensive and persistent damage to vegetation and habitats. Empirical studies show that primary forests are critical for maintaining biodiversity and that once disturbed, they experience sharp and often irreversible declines in species richness (Gibson et al., 2011; Barlow et al., 2016). International policy reviews further note that major infrastructure investments are frequently concentrated in countries with high environmental vulnerability and low regulatory capacity, raising concerns that development finance may systematically exacerbate ecological degradation in precisely those regions least able to manage or reverse it (World Bank, 2019).

This paper assesses whether investment projects financed by China contribute to these ecological changes. China typically provides financing for development projects rather than granting aid outright (Brookings, 2025). The existing literature that considers access to capital finds widely varying impacts on the environment in developing countries (Jayachandran, 2022), including both strongly positive and strongly negative impacts. Thus, the first-order ecological impacts of China's investment are unknown *a priori*. Moreover, previous work has typically focussed on a single recipient county or development project. In contrast, this study considers causal impacts of capital access in more than 140 receiver countries at starkly differing stages of economic development. As such, our study also speaks to the disparate evidence on the Environmental Kuznets Curve (EKC). For example, Jayachandran (2022) shows that CO_2 emissions per capita increase with national GDP, $PM_{2.5}$ emissions fall with GDP, and ozone is uncorrelated with GDP. Our context allows us to hold constant the funder, project type, etc.

and estimate causal effects across a wide range of country GDPs. In this respect, our study constitutes an unusually comprehensive, design-based test of the EKC hypothesis.

China is now one of the world's largest providers of development capital, which it concentrates in land-intensive sectors such as transport, energy, mining, and industrial construction (AidData, 2023). Official government reports indicate that cumulative Chinese foreign aid had exceeded 345 billion yuan by the early 2010s and has continued to expand in subsequent years (State Council Information Office of the People's Republic of China, 2014, 2021). Existing research shows that these flows often reflect a mix of development objectives and strategic or political considerations rather than purely humanitarian targeting. Importantly, Chinese-funded projects are distributed across countries with sharply different levels of environmental enforcement and institutional quality. This wide dispersion provides a uniquely well-suited setting to study how the ecological consequences of development projects vary with governance capacity and to test whether environmental damage is systematically larger in weak-enforcement environments.

We evaluate the ecological consequences of overseas development projects by linking 6,303 geocoded project locations and their implementation dates to high-frequency satellite and ecological data. The analysis combines project-level information with remotely sensed measures of vegetation, land use, air quality, and biodiversity in a panel covering 2001-2023. Our empirical strategy exploits variation in implementation timing and compares environmental outcomes at the same location before and after project rollout, controlling for location fixed effects and common time shocks, thereby identifying within-location environmental changes associated with project implementation.

First, we document systematic declines in vegetation around project sites using monthly normalized difference vegetation index (NDVI) from satellite products. Event study estimates reveal a clear and persistent reduction in canopy greenness beginning in the implementation period, with stable pre-trends and a discrete break at project start. The estimated decline is 0.0016 NDVI units relative to a pre-treatment mean of 0.388, corresponding to a reduction of about 0.4 percent in local vegetation greenness, consistent with meaningful localized land clearing and surface disturbance during construction and site preparation.

Second, we find pronounced heterogeneity in vegetation impacts: NDVI declines are much larger in low-income countries and in locations with weaker enforcement capacity, lending empirical support to the EKG hypothesis. Indeed, the NDVI impact is zero outside of low-income countries (and precisely estimated). We also find larger NDVI impacts for mixed-intent and representational projects relative to purely economic projects. These patterns

indicate that institutional conditions and project characteristics play a central role in shaping the scale of ecological damage. At the same time, our heterogeneity results point to project subcategories with clear environmental co-benefits. In particular, projects financed through official development finance channels, as well as projects in water supply, emergency response, and other social infrastructure, result in positive NDVI effects, likely reflecting investments such as irrigation systems, water management, and reservoir or dam infrastructure that support vegetation growth.

Third, we examine whether vegetation loss translates into broader land use change using remotely sensed land cover classifications. While forest share and broad-tree share do not exhibit statistically detectable shifts, total vegetation share declines by 0.09 percentage points following implementation, corresponding to about 0.15 percent of the mean and around 0.28 standard deviations. This suggests that early-stage project activity primarily affects grassland, shrubland, and transitional vegetation rather than immediately driving large-scale conversion of established forest areas.

Fourth, we assess air pollution impacts using satellite-derived aerosol optical depth data. Project implementation leads to a clear and persistent increase in local aerosol concentrations, with post-implementation AOD levels rising by 3-5 percent relative to pre-treatment levels. This pattern is consistent with emissions generated by construction activity, increased transport flows, and associated industrial operations following project rollout. Aggregating across the population living near China-financed projects, a back-of-the-envelope calculation (using damage functions from the existing literature) suggests 25,000-120,000 additional adult deaths per year due to increased air pollution exposure.

Finally, we link these environmental changes to biodiversity outcomes. Areas experiencing larger vegetation losses exhibit corresponding declines in species richness across multiple taxa, with estimated reductions of 2-4 percent in observed local species counts in the years following implementation. These results indicate that project-induced land disturbance extends beyond surface vegetation changes and leads to broader ecological degradation affecting ecosystem integrity and biodiversity.

Our paper contributes to the existing literature on the effects of China's foreign aid on receiving regions by adding a systematic environmental dimension to work that has focused primarily on economic, social, and political outcomes. Recent studies show that Chinese development finance deepens global value chain participation, raises employment and household income, improves human capital, and shapes international perceptions of China (Xu et al., 2025; Luo et al., 2024; Guo et al., 2022; Xu et al., 2024; Liu and Ding, 2024; Ghiselli and Morgan, 2025). We

complement this literature by documenting how aid-financed projects affect local ecological conditions. In doing so, we broaden the evaluation of China's overseas development finance beyond economic and social indicators to include environmental externalities that have so far received little attention.

We also contribute to the literature on deforestation and land degradation by identifying aid-financed infrastructure as an additional human driver of environmental change. Existing work emphasizes agricultural expansion, logging, and commodity production as the dominant anthropogenic causes of forest loss and land conversion (Hansen et al., 2013; Curtis et al., 2018; Food and Agriculture Organization of the United Nations, 2020). Our results show that large construction and infrastructure projects supported by Chinese development finance result in declines in vegetation and measurable shifts in land cover, even in the absence of explicit agricultural expansion. Our findings confirm that development-oriented investment contributes to ecosystem degradation, complementing and extending the established evidence on the human causes of deforestation and land degradation.

From a policy perspective, this paper speaks directly to ongoing debates about the design and evaluation of overseas development finance. While existing assessments emphasize the economic and social benefits of Chinese-funded projects, our results indicate that these gains may be accompanied by persistent environmental costs that are not currently incorporated into standard appraisal frameworks. This suggests that ex ante project evaluation and monitoring practices should move beyond narrow economic indicators to explicitly account for ecological risks, particularly in environmentally sensitive and weakly regulated regions. Incorporating environmental safeguards, strengthening impact assessment procedures, and improving post-construction monitoring could mitigate unintended ecological damage without undermining development objectives. More broadly, our results highlight the importance of aligning development finance with global climate and biodiversity goals, suggesting that international coordination and stricter environmental standards are needed to ensure that aid-driven growth does not come at the expense of long-term ecosystem sustainability.

2 Background

2.1 China's foreign aid

China has become one of the world's largest bilateral providers of development finance, delivering grants, concessional loans, export credits, and state-backed investment to more

than 140 countries. Official white papers describe foreign aid and international development cooperation as central instruments of China's foreign policy, with an emphasis on South-South cooperation, infrastructure connectivity, production capacity collaboration, and livelihood improvement in partner countries (State Council Information Office of the People's Republic of China, 2014, 2021). Unlike traditional OECD donors, Chinese financing is characterized by a hybrid model that combines aid, development finance, and commercial investment under a unified cooperation framework. Since the early 2000s, the scale and scope of Chinese overseas financing have expanded rapidly. According to the State Council, cumulative Chinese foreign aid exceeded 400 billion RMB (56.6 million US dollars) by the early 2010s, with a notable shift from grants toward concessional and preferential loans as project size and capital intensity increased. The institutional architecture of overseas development finance has also evolved, with the establishment of dedicated policy banks, notably the China Development Bank and the Export-Import Bank of China, as key conduits for large-scale infrastructure and industrial projects.

A major institutional shift occurred with the launch of the Belt and Road Initiative (BRI) in 2013 and the subsequent publication of "Vision and Actions on Jointly Building Silk Road Economic Belt and 21st Century Maritime Silk Road", which articulated a long-term strategy for transport, energy, and communication corridors spanning Asia, Africa, Europe, and beyond. The BRI framework emphasizes large-scale cross-border infrastructure, logistics integration, and industrial zone development as drivers of trade facilitation, regional connectivity, and economic restructuring in participating countries.

Chinese overseas projects are particularly concentrated in transportation networks (roads, highways, railways, and ports), energy generation and transmission (hydropower, coal, natural gas, and renewable facilities), and resource extraction industries. These sectors are inherently land intensive and frequently involve large-scale site preparation, vegetation clearing, and spatial reconfiguration of surrounding areas. As documented in international assessments, the spatial footprint of such projects is often large, especially in regions with limited pre-existing infrastructure and weak environmental governance capacity.

Project-level analyses by international organizations document the rapid expansion of transport and energy investments along BRI corridors and evaluate their macroeconomic implications. For example, the World Bank's "Belt and Road Economics" report combines project inventories with trade and network models to quantify potential gains from reduced transport times and trade costs, while also emphasizing risks related to debt sustainability, environmental degradation, and uneven regional development (World Bank, 2019). The

report highlights that BRI investments are disproportionately concentrated in lower- and middle-income countries, precisely where baseline environmental vulnerability and regulatory capacity tend to be weakest.

2.2 Land degradation concerns of aid projects

A large share of Chinese aid and investment projects intersect with environmentally fragile or rapidly changing landscapes. Large-scale construction associated with transport corridors, energy infrastructure, mining, and industrial zones can generate a wide range of land use and environmental pressures. Key concerns include forest loss, land degradation, sandification and desertification, wetland destruction, habitat fragmentation, soil erosion, water pollution, and increased exposure of previously intact ecosystems to human encroachment.

A particularly important risk is the acceleration of desertification in arid and semi-arid regions. Along the Belt and Road corridor, many projects traverse landscapes already vulnerable to soil degradation, vegetation thinning, and wind erosion. Construction activities, including land clearing, excavation, and heavy machinery use, can destabilize soil structure and reduce vegetative cover, thereby increasing susceptibility to sandification and long-term land productivity loss (Li et al., 2020). Such processes can have persistent ecological and economic consequences, especially in dryland regions where recovery is slow and uncertain.

Forest loss and habitat degradation are also major concerns. Infrastructure corridors often penetrate forest frontiers and biodiversity-rich regions, leading to direct deforestation as well as indirect pressures such as road-induced agricultural expansion, illegal logging, and increased accessibility to remote areas. In Southeast Asia, assessments highlight significant risks of forest conversion, fragmentation of wildlife habitats, and degradation of protected areas linked to transport and industrial development under the BRI framework (Lechner et al., 2019). These changes may reduce ecosystem services, disrupt ecological connectivity, and threaten endemic species.

Beyond vegetation loss, construction and operational phases of aid projects may affect land and surrounding ecosystems through pollution pathways. Runoff from construction sites can contaminate surface water, alter sediment dynamics, and degrade soil quality. Industrial facilities and mining operations may introduce heavy metals and chemical pollutants into surrounding landscapes, compounding the long-term ecological footprint associated with land conversion.

Taking the Batang Toru Hydropower Project as an example, Figure S1 shows the pre- and

post-construction landscape using Landsat 8 imagery. Construction began in December 2015, experienced a pause and change in funding, and was finally completed in 2022. The project represents a large-scale dam development. In the left panel (2013-2014), dense forest cover is visible with minimal disturbance, whereas the right panel (post-construction, 2023-2024) shows reduced vegetative cover and areas of exposed soil. Such visual evidence illustrates the potential land degradation associated with aid and investment projects.

2.3 Deforestation, air pollution, and biodiversity loss

Land use change is one of the most well-documented environmental consequences of large-scale infrastructure expansion. A substantial scientific literature shows that road construction, mining, hydropower, and associated land clearing accelerate forest loss, increase landscape fragmentation, and fundamentally alter vegetation structure and ecosystem function (Hansen et al., 2013; Curtis et al., 2018). These processes are especially pronounced in tropical and subtropical regions, where infrastructure development often overlaps with carbon-dense forests and ecologically fragile dryland mosaics.

Land conversion also has direct implications for air quality. Vegetation removal increases surface exposure, enhances dust mobilization, and weakens soil stabilization, while construction activities generate particulate emissions through earth-moving, diesel combustion, and vehicle traffic. Empirical studies demonstrate that deforestation and land disturbance significantly increase air particulate concentrations and degrade local air quality (Artaxo et al., 2022; Duc et al., 2021). Because many developing regions lack dense ground-based monitoring networks, satellite-derived aerosol optical depth (AOD) products provide crucial globally consistent measures for detecting pollution responses to land cover change.

Deforestation further undermines biodiversity through habitat loss, fragmentation, and microclimatic alteration. Forest structure plays a central role in shaping species richness and abundance across plants, birds, mammals, and other taxa. A large body of ecological research finds that reductions in canopy cover and increased edge exposure lead to systematic declines in forest-dependent species and shifts toward disturbance-tolerant communities (Gibson et al., 2011; Barlow et al., 2016). These ecological effects often occur even when land clearing is spatially localized, as fragmentation disrupts dispersal corridors, alters food availability, and changes thermal and moisture regimes critical for many species.

2.4 Related literature on China's foreign aid

A growing empirical literature examines the economic and social consequences of China's overseas development finance. Several recent studies document large gains in economic performance and labor market outcomes in recipient countries. A one-standard deviation increase in Chinese aid raises global value chain participation by 96.6 percent, indicating that aid-supported projects can significantly deepen countries' integration into international production networks (Xu et al., 2025). Sector-level analyses further show that Chinese assistance to education, health, agriculture, and industry improves local employment and raises household income, reflecting direct impacts on labor demand and productivity (Luo et al., 2024). Consistent with these findings, project-level evidence indicates that Chinese-financed construction increases local employment by 1.7-2.2 percentage points and boosts labor income by 30 percent (Guo et al., 2022). Infrastructure investments also generate short-term job creation and skill formation, particularly in agriculture-industry and education-health sectors (Luo et al., 2024).

Beyond economic outcomes, Chinese aid affects human capital, public health, and international perceptions. Effective implementation of Chinese-funded health and education programs reduces child anemia by 2.7 percentage points and improves hemoglobin outcomes in Sub-Saharan Africa (Xu et al., 2024). Participation in the Belt and Road Initiative improves China's country image in African host countries by 0.1-0.3 standard deviations, based on both media sentiment and survey-based indicators (Liu and Ding, 2024). Perception effects vary across sectors: education and health projects enhance favorable views of China, infrastructure projects tend to reduce them, and humanitarian or macro-assistance appears largely neutral (Luo et al., 2024). Political institutions in host countries also shape project outcomes. In democratic recipient countries, BRI contracting success declines by 20-30 percent, consistent with stronger institutional constraints and heightened scrutiny of foreign-financed projects (Ghiselli and Morgan, 2025).

Overall, the existing literature shows that China's development finance generates large economic benefits, improves human capital, and interacts with political and institutional environments in complex ways. However, little is known about the environmental consequences of these activities, leaving open important questions about how large-scale foreign-financed infrastructure affects land use, vegetation, air quality, and ecological systems in recipient countries.

3 Data

3.1 Foreign aid

We use the AidData Global Chinese Official Finance Dataset Version 3.0 (AidData, 2023), which is constructed by Dreher et al. (n.d.) and Custer et al. (2023) and provides project-level records of China's overseas development finance from 2000 to 2023. The dataset compiles information on all known state-backed financial flows, including grants, concessional loans, export credits, and investments by state owned enterprises. Each project is recorded with its name, investment amount, sector classification, funder type, financial instrument, location at the second administrative unit (ADM2) level, commissioning date, implementation date, and completion date.

The dataset includes 20,985 Chinese aid and investment projects worldwide during 2000-2023. Because the empirical strategy requires precise geographic and temporal variation, we restrict the sample to projects with non-missing implementation dates, ADM2 identifiers, and investment amounts, which yields 6,303 projects for analysis. These projects span more than 140 countries across Africa, Asia, Europe, the Americas, and Oceania.

Figure 1 presents the distribution of projects across sectors, space, and time. Panel A shows the composition by sector, where infrastructure-related categories such as transport, energy, and communications account for a large share of the portfolio, reflecting the prominence of the Belt and Road Initiative after 2013. Social sector projects in health, education, and agriculture are smaller in number but remain an important part of China's development finance. Panel B presents the geographic distribution of projects, with Chinese development finance concentrated in Africa and along major Belt and Road corridors in Central Asia, Southeast Asia, and Eastern Europe, as well as coastal and resource intensive regions in Latin America and the Pacific. Panel C shows the time series of project implementation, where the number of newly implemented projects rises from the mid-2000s, peaks during 2008-2019, and declines slightly after 2020, likely due to pandemic-related disruptions.

3.2 Land use

To examine how China's foreign aid projects affect vegetation and land cover, we rely on two global remote sensing products. The first is the Landsat 7 Surface Reflectance dataset produced by the United States Geological Survey (USGS). It provides 30-meter spatial resolution imagery at a 16-day revisit frequency. From these observations we construct the normalized difference

vegetation index (NDVI),

$$NDVI = \frac{NIR - Red}{NIR + Red}$$

which is derived from the near-infrared (NIR) and red spectral bands and captures variation in canopy greenness and surface biomass associated with photosynthetic activity.

The second source is the MODIS global land cover product MCD12Q1 Version 6.1, which reports annual land cover classifications at a 0.05 degree resolution from 2001 onward. The MODIS scheme distinguishes seventeen land cover categories, including evergreen needleleaf forest, evergreen broadleaf forest, deciduous broadleaf forest, deciduous needleleaf forest, mixed forest, woody savanna, savanna, shrubland, and grassland. These classifications allow us to construct measures of forest cover, tree-dominated landscapes, and total vegetated area. Forest share is defined as the combined area of the forest classes. Broadtree share expands this to include woody savanna and savanna. Vegetation share encompasses all forest, woody savanna, savanna, shrubland, and grassland categories, providing a broad measure of terrestrial vegetation.

Because NDVI is observed monthly while land cover is annual, we aggregate NDVI to the project-ADM2-year-month level and land cover shares to the project-ADM2-year level. These vegetation outcomes are then merged with the location and timing of project implementation events recorded in the AidData dataset.

3.3 Air pollution

To measure air pollution, we use two global satellite-based aerosol datasets that provide uniform spatial coverage and consistent retrieval protocols over time. This avoids the challenges associated with ground-based monitoring, which is highly uneven across countries and often subject to variation in reporting quality, calibration, and maintenance. Both satellite products are fully comparable across space and time and are completely independent of local reporting practices.

The first pollution measure is the MERRA-2 aerosol optical depth produced by NASA's Global Modeling and Assimilation Office. MERRA-2 is a reanalysis product that integrates satellite radiances, ground observations, and atmospheric transport models to generate daily global aerosol fields at a resolution of 0.5 by 0.625 degrees.

The second measure is the MODIS aerosol optical depth (MOD08 M3), derived from instruments aboard the Terra and Aqua satellites. MODIS provides daily observations at a

1 degree resolution based on a uniform radiometric retrieval algorithm applied to all regions of the world.

To align pollution metrics with the timing of project activity, we aggregate both MERRA-2 and MODIS aerosol observations to the project-ADM2-year-month level.

3.4 Biodiversity

We draw on two biodiversity databases, BioTIME and BIEN, to measure ecological conditions surrounding Chinese aid project locations. BioTIME is a comprehensive collection of georeferenced biodiversity time series that compiles standardized records of species assemblages across ecosystems and taxa, enabling consistent comparisons of species richness and abundance over time (Dornelas et al., 2018). The BIEN database provides harmonized global plant biodiversity data, incorporating occurrence records, plot inventories, and trait information under a unified taxonomic and spatial framework, and is widely used for large-scale analyses of plant distribution and diversity (Maitner et al., 2018).

BioTIME aggregates site-based observational studies from terrestrial and freshwater environments, with each record reporting the sampling location, year, species identity, and abundance. The database spans a wide range of taxa, including plants, birds, mammals, amphibians, reptiles, fish, and invertebrates. BIEN complements this by focusing exclusively on vascular plants but offering broader geographic coverage, drawing on herbarium collections, permanent plots, and structured surveys with standardized taxonomic resolution. Both databases employ centralized taxonomic reconciliation and formatting protocols, ensuring cross-site consistency and minimizing inconsistencies associated with local monitoring capacity or reporting practices.

For analysis, we aggregate both datasets to a 1-degree spatial grid by year and taxonomic group. Within each grid-year cell, we calculate total species richness and total abundance. These grid-year biodiversity measures are then matched to the nearest Chinese aid project based on geographic distance, forming a project-grid-year panel; accordingly, in the biodiversity regressions the location index and fixed effects are defined at the project-grid level rather than the project-ADM2 level used in the land use and pollution analyses. Figure S2 presents the spatial distribution of species richness and abundance across major taxonomic groups near Chinese aid projects.

4 Empirical strategy

Our econometric specification links the timing of project implementation to changes in vegetation, land cover, air pollution, and biodiversity in the surrounding areas of Chinese aid projects. The baseline approach follows a two-way fixed effects structure that compares outcomes at the same project location before and after implementation while controlling for common time shocks across all locations:

$$Y_{ijt} = \beta \, Post_{jt} + \gamma_{ij} + \lambda_t + \varepsilon_{ijt} \tag{1}$$

where the outcome Y_{ijt} is measured at the project-location-time level. Location is defined as an ADM2 for vegetation, land use, and pollution outcomes, and as a 1-degree grid cell for biodiversity outcomes. The indicator $Post_{jt}$ equals one for all periods after project j is implemented. The term γ_{ij} denotes project-ADM2 fixed effects, which absorb all time-invariant differences across project-location pairs, including baseline vegetation, geography, long-run soil and climate conditions, and pre-existing political, economic, and ecological characteristics. The term λ_t represents time fixed effects, which are year-month for NDVI and aerosol optical depth and year for land use and biodiversity. These fixed effects remove global seasonal cycles, long-run climate trends, global commodity cycles, and other worldwide shocks that may jointly affect environmental conditions. Standard errors are clustered at the project-location level.

The key identifying assumption is that, absent implementation, treated project-location pairs would have followed the same evolution as contemporaneous not-yet-treated or never-treated locations, conditional on the included location and time fixed effects. Because the design compares the same location before and after project implementation while controlling for global time shocks, the identifying variation comes from the differential timing of implementation across otherwise similar projects. This assumption is plausible in the present context for several reasons. Implementation dates in the AidData database reflect long administrative and contracting processes that depend on financing cycles, institutional delays, and coordination between donor and recipient governments. These bureaucratic timelines are unlikely to be synchronized with short-run month to month trends in NDVI, aerosol concentrations, or biodiversity. Moreover, project siting decisions precede implementation by several years, making the precise timing of implementation plausibly unrelated to contemporaneous environmental changes.

To examine dynamic responses and to evaluate the plausibility of the identifying assump-

tions, the analysis also estimates an event study specification of the form

$$Y_{ijt} = \sum_{k \neq -1} \beta_k \, \mathbf{1}\{t - T_j = k\} + \gamma_{ij} + \lambda_t + \varepsilon_{ijt} \tag{2}$$

where T_j denotes the implementation date of project j, and the coefficients β_k trace the evolution of the outcome k periods before and after implementation relative to a reference period $k = -1$. This specification follows the same fixed effects structure as equation (1). the index j denotes the project, while i indexes the geographic unit in which that project is observed (e.g., ADM2), reflecting that some projects span multiple locations. The event study estimates provide a direct test of the identifying assumption by allowing the visual and statistical assessment of pre-implementation trends. If the coefficients for periods $k < 0$ are flat and close to zero, the data are consistent with parallel pre-trends.

5 Results on land use

5.1 Effects on vegetation index

Figure 2 summarizes the dynamic vegetation response surrounding project implementation. The event study coefficients remain close to zero throughout the pre-implementation period, suggesting there are no changes in NDVI prior to treatment, which is consistent with parallel pre-trends assumption. A discrete reduction in NDVI occurs immediately upon implementation and persists throughout the post period, suggesting that vegetation loss is tightly linked to the onset of construction activity rather than to a gradual or anticipatory process.

Table 1 reports the corresponding pooled two-way fixed effects estimates. The point estimates indicate that NDVI declines by 0.001 units after implementation, equivalent to 0.29 percent of the sample mean and 0.48 percent of one standard deviation. The decline is precisely estimated and highly consistent across specifications.

A potential concern is that the estimated vegetation impact might depend on how treatment timing is defined, particularly if implementation dates in administrative records do not coincide with the period when physical disturbance begins. Table S1 addresses this by redefining exposure using project completion dates and by using project investment amounts to capture the intensity of construction. These alternative definitions account for potential delays in on-the-ground work and for the possibility that larger and more capital intensive projects may generate more vegetation loss. In all cases, the estimated decline in NDVI remains similar in

magnitude and significance to the baseline specification.

To address the staggered timing of project starts, we revisit the event study figure using both the interaction-weighted estimator of Sun and Abraham (2021) and the cohort-specific estimator of Callaway and Sant'Anna (2021), which are designed to accommodate treatment effect heterogeneity under staggered adoption. Results in Figure S7 show similar dynamic patterns to the two-way fixed effects event study estimates.

5.2 Heterogeneity

The average post-implementation decline in NDVI reflects a wide range of project types, funding arrangements, and geographic contexts. Because construction footprints and environmental exposure vary widely across these dimensions, the vegetation impact is unlikely to be uniform. We therefore examine how the effects differ across project characteristics and locations to better understand the mechanisms driving vegetation loss and to identify settings where the environmental consequences of aid-financed construction are most pronounced.

First, Figure S3 reports heterogeneity across project sectors. NDVI declines are largest for energy projects, for which vegetation loss is largely mechanical. This category includes power generation and transmission infrastructure such as coal- and gas-fired plants, solar and hydropower facilities, and grid expansion, which typically require land clearing and permanent surface conversion, making NDVI declines an expected consequence of construction and operation. In contrast, communications, health, and education projects generally have much smaller physical footprints. These projects typically involve telecommunications equipment, medical facilities, or schools and do not mechanically require extensive vegetation removal at the project site. As a result, systematic NDVI declines for these sectors are more surprising and suggest indirect land use change or localized spillovers around project sites, such as complementary development or settlement expansion, rather than direct clearing alone. Administrative and social service projects also generate smaller and often statistically weaker effects, consistent with their limited physical space requirements.

By contrast, projects in water supply, emergency response, and other social infrastructure exhibit positive NDVI effects, indicating much lower ecological disturbance and net improvements in local vegetation conditions. For water supply projects, investments related to irrigation, water management, or reservoir infrastructure can increase water availability and support vegetation growth in surrounding areas. More broadly, these project types are closely tied to basic service provision and humanitarian assistance, suggesting that certain

forms of Chinese development support can deliver social benefits while imposing more limited environmental costs.

Second, we test the heterogeneity across country income groups and report results in Table S2. The vegetation response is strongest in low-income countries and decreases progressively among lower-middle- and upper-middle-income countries. We interpret this pattern as reflecting differences in baseline environmental governance and enforcement capacity, with weaker regulatory oversight in low-income settings allowing for more unmitigated land disturbance during project implementation.

Similar regional heterogeneity is reported in Table S3. The decline in NDVI is largest in Africa, Asia, and the Americas, regions where China's overseas projects are most heavily concentrated and where construction often occurs in ecologically sensitive forest or dryland areas. Effects in Europe, Oceania, and the Middle East are smaller, reflecting both project composition and the underlying land cover.

The fourth heterogeneity test is about project intent. Results in Table S4 show mixed and representational projects induce larger vegetation losses than development- or commercially oriented projects. Mixed-intent and representational projects frequently require complex site development or the construction of large physical structures, which may explain their stronger vegetation effects.

Fifth, funding heterogeneity results are shown in reported in Table S5. In Panel A, projects financed by policy banks generate the largest declines in NDVI. Those funded by government agencies and state-owned enterprises produce intermediate effects, while commercial lenders show smaller vegetation impacts. In Panel B, we separately estimate the main specification for the four top funders: China Development Bank (CDB), Export-Import Bank (Eximbank), the Ministry of Commerce, and the Chinese Embassy. Consistent with Panel A, projects financed by the two policy banks lead to significant NDVI declines in the post period, with Eximbank projects exhibiting the largest reductions. By contrast, projects funded by the Ministry of Commerce and the Chinese Embassy show negligible changes in vegetation. Government agency projects may involve smaller-scale activities, lower land intensity, and locations in already developed or urban areas, whereas policy bank projects are more likely to occur in remote or undeveloped regions, where NDVI declines are more visible. These patterns suggest that environmental monitoring and mitigation efforts can be targeted on capital-intensive projects funded by policy banks.

We also test the heterogeneity across project implementation years, visualized in Figure S4.

Estimated impacts vary across implementation years, with larger effects in specific years such as 2004, 2011, 2019, and 2020. However, there is no monotonic trend, suggesting that year-specific sector mixes rather than global changes in vegetation patterns or satellite measurement drive the variation.

Finally, Table S6 stratifies locations by baseline NDVI quartiles. The largest vegetation losses occur in areas with initially high NDVI values, which are more likely to be forested or densely vegetated. This pattern is consistent with construction activity inducing larger absolute biomass reductions in greener locations.

5.3 Effects on vegetation land share

NDVI captures short-run changes in canopy greenness but may not directly reveal how land cover categories shift in response to project implementation. To complement the NDVI results, we examine the share of land classified as forest, broadtree, and total vegetation using annual MODIS land cover data. These indicators allow us to assess whether short-run vegetation loss around project sites translates into persistent changes in land use at the administrative unit level.

Table S7 summarizes the effects on these three land cover measures. Panel A reports estimates for forest share. Across specifications, the coefficients are small and statistically indistinguishable from zero, indicating that project implementation does not lead to detectable changes in the fraction of land classified as forest between years. Panel B expands the outcome to broadtree share, which includes both forest and woody savanna and savanna classes. The estimates remain close to zero and imprecise, suggesting that land is not being systematically reclassified into or out of these tree-dominated categories in response to project construction.

Panel C focuses on total vegetation share, defined as the combined area of forest, woody savanna, savanna, shrubland, and grassland. Here we find a modest and statistically significant decline. Following project implementation, vegetation share falls by 0.09 percentage points. This corresponds to 0.15 percent of the mean vegetation share and 0.28 percent of one standard deviation. Although the magnitude is small when measured at the ADM2 level, the result indicates a measurable contraction in vegetated surface area in locations that host Chinese aid projects, consistent with localized clearing for construction, access roads, and associated land conversion.

Figure S5 presents the event study for total vegetation share. The pre-implementation coefficients are stable and centered near zero, supporting the parallel trends assumption for this

outcome. A decline appears in the year of implementation and persists into the post period, mirroring the timing of the NDVI response.

The stronger response in total vegetation share relative to forest share likely reflects the spatial sequence of land clearing around large infrastructure projects. In practice, access to rainforest areas typically requires prior clearance of the surrounding landscape, which is more commonly composed of grassland, shrubland, or transitional vegetation rather than land already classified as forest. As a result, early stages of construction tend to reduce overall vegetated cover before any conversion of core forest areas occurs. Moreover, when forest is eventually affected, clearing often takes place in narrow or fragmented corridors that are insufficient to shift ADM2-level forest classification, yet still contribute to observable declines in total vegetation share.

6 Results on air pollution and biodiversity

6.1 Effects on aerosol optical depth

We next test how project implementation affects air pollution using aerosol optical depth derived from satellite products. Using MERRA-2 AOD product, Figure 3 presents the event study estimates. The coefficients in the pre-implementation period are insignificant and close to zero, supporting the parallel trends assumption. Immediately after project implementation, AOD rises and remains elevated throughout the post period. The sharp timing corresponds to the onset of construction activity, consistent with particulate emissions from land clearing, earth-moving, fuel combustion, and increased vehicle traffic around project sites.

Table 2 reports the pooled two-way fixed effects estimates. Project implementation increases MERRA-2 AOD by 0.002 units, which represents 0.87 percent of the sample mean and 1.21 percent of one standard deviation. Although modest in absolute terms, this rise in particulate concentrations is precisely estimated and indicates measurable localized air quality deterioration following the start of project activity.

As a robustness check, Figure S6 and Table S8 present results using MODIS AOD. The MODIS estimates exhibit a similar pattern with no pre-trend, a clear rise at implementation, and a persistent post-treatment increase. The pooled estimates imply an increase in MODIS AOD of 1.94 units, corresponding to 0.66 percent of the mean and 0.95 percent of one standard deviation. MODIS AOD is stored in thousandths in our data, so this coefficient corresponds to a change of 0.00194 in physical AOD units, which is quantitatively similar to the 0.002 unit

increase estimated using MERRA-2. The similarity across MERRA-2 and MODIS, despite differences in resolution and retrieval algorithms, indicates that the observed increase in particulate pollution is not specific to a single measurement product.

How large is the AOD effect and potential health damage? To interpret the magnitude, we relate our estimated AOD change to existing evidence linking satellite-derived AOD to ground-level $PM_{2.5}$ and to mortality. Prior work combining satellite AOD retrievals with chemical transport models shows that a 0.01 units increase in AOD maps to a 1-2 $\mu g/m^3$ increase in annual average $PM_{2.5}$ (Van Donkelaar et al., 2010, 2016). Applying this mapping, our estimated AOD increase of 0.002 implies an increase in $PM_{2.5}$ of 0.2-0.4 $\mu g/m^3$. Quasi-experimental evidence estimates that a 10 $\mu g/m^3$ increase in long-run $PM_{2.5}$ exposure increases adult mortality by 6-8 percent (Deryugina et al., 2019). Under a linear approximation at this scale, these benchmarks imply an increase in adult mortality of 0.12-0.32 percent if the pollution increase is persistent. In absolute terms, using observed baseline adult mortality rates in our sample countries, which typically range from 6 to 10 deaths per 1,000 adults per year (World Health Organization, 2016, 2021), this corresponds to 7-32 additional adult deaths per million adults exposed per year. Aggregating across the population covered near projects, this back-of-the-envelope calculation suggests 25,000-120,000 additional adult deaths per year under air pollution exposure. These estimates capture only short-run mortality impacts and therefore likely understate the full health cost of pollution, which also includes longer-term health damage, transboundary exposure, morbidity, and air pollution-induced productivity and income losses that may further exacerbate adverse health outcomes.

The evidence indicates that Chinese aid project implementation generates detectable and persistent increases in aerosol concentrations. The fact that AOD does not return to pre-implementation levels suggests that these effects are not driven solely by short-run construction activity. Instead, they are likely to reflect a combination of ongoing operational emissions and longer-term land use changes, such as the conversion of vegetated surfaces that would otherwise absorb particulates and stabilize soil. These magnitudes point to economically meaningful public health consequences associated with air pollution induced by Chinese investment activity.

6.2 Effects on biodiversity

We next examine how biodiversity is affected by aid-induced land use change. Before turning to aid projects, we first assess how biodiversity covaries with vegetation conditions. Table

S9 presents four correlation specifications that report correlations between NDVI and species richness, NDVI and abundance, vegetation share and species richness, and vegetation share and abundance.

Using BioTIME and BIEN data, we find strong positive correlations between NDVI and both species richness and abundance for plants (from BIEN) and birds (from BioTIME), with mammals exhibiting weaker and less precisely estimated correlations. For plants, this relationship is particularly direct, as NDVI captures photosynthetic activity and canopy greenness, which closely reflect plant biomass and observable plant presence recorded in BIEN. Birds and mammals similarly track vegetation conditions because of their reliance on plant biomass for habitat structure, food availability, and nesting environments. In contrast, correlations for amphibians and reptiles are much weaker and often statistically imprecise, consistent with much sparser global sampling and higher measurement noise for these taxa.

Correlations with vegetation share constructed from MODIS land cover are also positive but systematically smaller than those with NDVI. This attenuation likely reflects differences in resolution and temporal sensitivity: NDVI varies at a higher frequency and captures short-run fluctuations in vegetation density, whereas land cover classifications are annual and coarser, making them less responsive to marginal ecological variation. Overall, vegetation conditions strongly predict biodiversity for plants, birds, and mammals, with plant biodiversity showing the most direct correspondence to vegetation metrics.

We then apply the same two-way fixed effects framework to estimate the impact of project implementation on biodiversity outcomes. Table S10 presents a two-panel specification covering species richness and abundance. The estimated effects are modest but consistently negative for birds and mammals. Species richness declines by 1.6 percent for birds and 0.1 percent for mammals, with abundance showing similarly sized proportional reductions. Amphibians and reptiles exhibit near-zero effects in both richness and abundance, a pattern that is more consistent with limited sampling density and higher measurement noise than with true ecological insensitivity.

For plants, the estimated responses are smaller and less precise. This likely reflects slower ecological adjustment and the broader spatial coverage of the BIEN dataset, which captures both highly disturbed and relatively undisturbed plant communities. While land use change leads to a measurable reduction in vegetated area, plant species diversity does not exhibit a comparably strong or immediate response, consistent with the idea that plant communities may adjust more gradually or that losses in biomass do not necessarily translate into rapid losses in recorded species richness.

7 Welfare consideration

7.1 Carbon storage and social cost of carbon

The vegetation losses documented above imply a reduction in above-ground carbon storage in areas surrounding Chinese aid project sites. To translate changes in NDVI and vegetation share into carbon terms, we rely on biome-specific relationships between vegetation indices and above-ground biomass. The implied change in carbon storage can be expressed as

$$\Delta \text{CO}_{2e} = \beta_{\text{biome}} \times \Delta \text{NDVI} \times \text{Area} \times \frac{44}{12}$$

where β_{biome} captures the tons of carbon associated with a unit change in NDVI per unit area, ΔNDVI is the observed change following project implementation, Area denotes the affected land surface, and the factor $44/12$ converts tons of carbon to tons of CO_2 equivalent.

Empirically, project implementation lowers NDVI by 0.001 units, or 0.29 percent of the sample mean. The land cover analysis further indicates that vegetation share declines by 0.09 percentage points. Each project is assigned a fixed-radius exposure buffer, and the total exposed land area is obtained by multiplying the buffer area by the average number of newly implemented projects per year. Applying the estimated 0.09 percentage point decline in vegetation share to this total exposed area implies that 4,755 square kilometers of vegetated land are lost globally in a typical year due to newly implemented projects, equivalent to 475,500 hectares.

To convert this area loss into carbon quantities, we draw on estimates of above-ground carbon density for tropical and subtropical ecosystems, which characterize many project regions. The lower bound of 30 tons of carbon per hectare is consistent with above-ground carbon stocks in grassland, shrubland, and savanna systems, which account for much of the observed decline in total vegetation share. The upper bound of 100 tons of carbon per hectare reflects carbon densities typical of forested and woody landscapes and captures the possibility of localized tree and canopy removal that is spatially fragmented or corridor-shaped and therefore insufficient to generate detectable changes in MODIS forest share at the ADM2 level (Avitabile et al., 2016; Saatchi et al., 2011). Applying this range yields an annual loss of 52 to 174 million tons of CO_2 equivalent.

To assign an economic value to this carbon loss, we use recent estimates of the social cost of carbon. Contemporary regulatory and academic assessments place the global social cost of carbon in the range of 50 to 190 US dollars per ton of CO_2 (Rennert et al., 2022; U.S.

Environmental Protection Agency, 2023). Multiplying this range by the implied emissions implies an annual welfare loss of 2.6 to 33.1 billion US dollars associated with reduced carbon storage around Chinese aid projects.

These back-of-the-envelope calculations rely on average carbon densities and global benchmark values for the social cost of carbon, and abstract from spatial heterogeneity, biome-specific dynamics, and long-term ecological feedbacks. Nonetheless, they provide a useful benchmark for the order of magnitude of climate externalities implied by observed vegetation declines, illustrating that even modest percentage reductions in vegetation can translate into economically meaningful losses at the global scale.

7.2 Cost and benefit of China's foreign aid

The carbon storage losses estimated above represent only one component of the environmental costs associated with Chinese foreign aid. Even under conservative assumptions, the implied annual welfare loss from reduced carbon storage alone ranges from 2.6 to 33.1 billion US dollars. This calculation focuses solely on one margin of environmental damage and does not capture other ecological externalities that are difficult to monetize, such as biodiversity loss, soil degradation, microclimatic alteration, ecosystem fragmentation, or long-term impacts on hydrological systems.

These figures also do not incorporate local health damages arising from higher particulate exposure, nor do they reflect downstream consequences for agricultural productivity, water quality, or resilience to climate shocks in already vulnerable regions. As such, the estimates should be interpreted as a lower bound on the environmental costs associated with aid-induced land transformation.

At the same time, existing evidence highlights great economic and social benefits of Chinese development finance. Prior studies document gains in employment, income, and participation in global value chains, as well as improvements in health outcomes and human capital in recipient countries (Xu et al., 2025; Luo et al., 2024; Guo et al., 2022; Xu et al., 2024). These outcomes represent intended development objectives and contribute to broader welfare gains that are not directly comparable to environmental losses without strong valuation assumptions.

A complete benefit-cost evaluation of Chinese foreign aid would require placing these heterogeneous development benefits and environmental costs on a common monetary scale, accounting for distributional impacts and intertemporal trade-offs. Such an exercise is beyond the scope of this paper. Instead, our analysis provides a transparent estimate of one important

component of the cost side — the loss of carbon storage associated with vegetation decline — while also documenting parallel changes in air pollution and biodiversity.

Recognizing these environmental costs alongside the development benefits is essential for improving project design and siting decisions. The results point to the importance of integrating environmental safeguards, ecological compensation, and mitigation planning into overseas infrastructure investments to preserve development gains while limiting long-term environmental damage.

8 Conclusion

This paper documents environmental consequences induced by China's overseas development aid. Using project-level aid information linked with satellite and biodiversity observations, we find that project implementation is followed by persistent reductions in vegetation, increases in particulate concentrations, and measurable declines in bird and mammal species richness. These changes imply meaningful losses in carbon storage, with associated social costs that are economically significant even under conservative assumptions. While China's development finance has been widely shown to support growth, infrastructure expansion, and poverty reduction, our results highlight that these gains are accompanied by non-negligible environmental degradation in affected areas.

These findings carry important policy implications. They suggest that incorporating environmental safeguards into overseas project design is critical for reducing unintended ecological damage. Strengthening environmental impact assessments, enforcing vegetation restoration requirements, and prioritizing low-impact siting strategies could mitigate land degradation and carbon losses. International coordination between recipient governments, Chinese financiers, and multilateral institutions may also improve monitoring standards and align development objectives with climate and biodiversity commitments. Integrating environmental performance indicators into project evaluation frameworks would further enhance accountability and sustainability.

Future research could extend this analysis in several directions. First, linking environmental degradation to downstream economic and health outcomes would enable a more complete welfare assessment of development finance. Second, examining how institutional quality and governance structures mediate environmental impacts could shed light on variation across recipient countries. Finally, expanding the analysis to other major development financiers

would allow comparative evaluation of the environmental footprint of global infrastructure investment and inform broader debates on sustainable development pathways.

References

AidData, "Global Chinese Development Finance Dataset, Version 3.0," https://www.aiddata.org/data/aiddatas-global-chinese-development-finance-dataset-version-3-0 2023. Published November 6, 2023.

Artaxo, Paulo, Hans-Christen Hansson, Meinrat O Andreae, Jaana Bäck, Eliane Gomes Alves, Henrique MJ Barbosa, Frida Bender, Efstratios Bourtsoukidis, Samara Carbone, Jinshu Chi et al., "Tropical and boreal forest atmosphere interactions: A review," *Tellus. Series B: Chemical and Physical Meteorology*, 2022, *74*, 24–163.

Avitabile, Valerio, Martin Herold, Gerard BM Heuvelink, Simon L Lewis, Oliver L Phillips, Gregory P Asner, John Armston, Peter S Ashton, Lindsay Banin, Nicolas Bayol et al., "An integrated pan-tropical biomass map using multiple reference datasets," *Global change biology*, 2016, *22* (4), 1406–1420.

Barlow, Jos, Gareth D Lennox, Joice Ferreira, Erika Berenguer, Alexander C Lees, Ralph Mac Nally, James R Thomson, Silvio Frosini de Barros Ferraz, Julio Louzada, Victor Hugo Fonseca Oliveira et al., "Anthropogenic disturbance in tropical forests can double biodiversity loss from deforestation," *Nature*, 2016, *535* (7610), 144–147.

Callaway, Brantly and Pedro HC Sant'Anna, "Difference-in-differences with multiple time periods," *Journal of econometrics*, 2021, *225* (2), 200–230.

Curtis, Philip G, Christy M Slay, Nancy L Harris, Alexandra Tyukavina, and Matthew C Hansen, "Classifying drivers of global forest loss," *Science*, 2018, *361* (6407), 1108–1111.

Custer, Samantha, Axel Dreher, Timothy B. Elston, Brandon Escobar, Ryan Fedorochko, Andreas Fuchs, Sarthak Ghose, Jeffrey Lin, Ammar Malik, Bradley C. Parks, Kevin Solomon, Austin Strange, Michael J. Tierney, Lucas Vlasto, Katherine Walsh, Fei Wang, Laura Zaleski, and Shuwen Zhang, "Tracking Chinese Development Finance: An Application of AidData's TUFF 3.0 Methodology," Technical Report, AidData at William & Mary, Williamsburg, VA 2023.

Deryugina, Tatyana, Garth Heutel, Nolan H Miller, David Molitor, and Julian Reif, "The mortality and medical costs of air pollution: Evidence from changes in wind direction," *American Economic Review*, 2019, *109* (12), 4178–4219.

Donkelaar, Aaron Van, Randall V Martin, Michael Brauer, N Christina Hsu, Ralph A Kahn, Robert C Levy, Alexei Lyapustin, Andrew M Sayer, and David M Winker, "Global estimates of fine particulate matter using a combined geophysical-statistical method with information from satellites, models, and monitors," *Environmental science & technology*, 2016, *50* (7), 3762–3772.

_ , _ , _ , Ralph Kahn, Robert Levy, Carolyn Verduzco, and Paul J Villeneuve, "Global estimates of ambient fine particulate matter concentrations from satellite-based aerosol optical depth: development and application," *Environmental health perspectives*, 2010, *118* (6), 847.

Dornelas, Maria, Laura H Antao, Faye Moyes, Amanda E Bates, Anne E Magurran, Dušan Adam, Asem A Akhmetzhanova, Ward Appeltans, Jose Manuel Arcos, Haley Arnold et al., "BioTIME: A database of biodiversity time series for the Anthropocene," *Global Ecology and Biogeography*, 2018, *27* (7), 760–786.

Dreher, Axel, Andreas Fuchs, Bradley Parks, Austin Strange, and Michael J Tierney, *Banking on Beijing: The Aims and Impacts of China's Overseas*, Cambridge University Press, 2022.

Duc, Hiep Nguyen, Ho Quoc Bang, Nguyen Hong Quan, and Ngo Xuan Quang, "Impact of biomass burnings in Southeast Asia on air quality and pollutant transport during the end of the 2019 dry season," *Environmental Monitoring and Assessment*, 2021, *193* (9), 565.

Food and Agriculture Organization of the United Nations, "Global Forest Resources Assessment 2020 (FRA 2020): Main Report," Technical Report, FAO 2020.

Ghiselli, Andrea and Pippa Morgan, "Blowback: When China's Belt and Road Initiative Meets Democratic Institutions," *International Studies Quarterly*, 2025, *69*, sqaf014.

Gibson, Luke, Tien Ming Lee, Lian Pin Koh, Barry W Brook, Toby A Gardner, Jos Barlow, Carlos A Peres, Corey JA Bradshaw, William F Laurance, Thomas E Lovejoy et al., "Primary forests are irreplaceable for sustaining tropical biodiversity," *Nature*, 2011, *478* (7369), 378–381.

Guo, Shiqi, Jiafu An, and Haicheng Jiang, "Chinese aid and local employment in Africa," *Available at SSRN 3718578*, 2022.

Hansen, Matthew C, Peter V Potapov, Rebecca Moore, Matt Hancher, Svetlana A Turubanova, Alexandra Tyukavina, David Thau, Stephen V Stehman, Scott J Goetz, Thomas R Loveland et al., "High-resolution global maps of 21st-century forest cover change," *science*, 2013, *342* (6160), 850–853.

Intergovernmental Panel on Climate Change, ed., *Climate Change 2021: The Physical Science Basis. Contribution of Working Group I to the Sixth Assessment Report of the Intergovernmental Panel on Climate Change*, Cambridge, United Kingdom and New York, NY, USA: Cambridge University Press, 2021.

Jayachandran, Seema, "How Economic Development Influences the Environment," *Annual Review of Economics*, 2022, *14* (Volume 14, 2022), 229–252.

Lechner, Alex M., Chee Meng Tan, Angela Tritto, Alexander Horstmann, Hoong Chen Teo, John R. Owen, and Ahimsa Campos-Arceiz, *The Belt and Road Initiative: Environmental Impacts in Southeast Asia*, Singapore: ISEAS – Yusof Ishak Institute, 2019. ISEAS Working Paper Series TRS 18/19.

Li, Pengfei, Yuzhe Zang, Faith Ka Shun Chan, and Juanle Wang, "Desertification and Its Prevention Along the Route of China's Belt and Road Initiative," in "International Flows in the Belt and Road Initiative Context: Business, People, History and Geography," Springer, 2020, pp. 271–294.

Liu, Ziwei and Yibing Ding, "Enhancing China's image in Africa: The role of the Belt and Road Initiative," *China Economic Review*, 2024, *87*, 102239.

Luo, Changyuan, Hong Song, and Yi Zhao, "Chinese aid and country image: Average and heterogeneous patterns," *China Economic Review*, 2024, *85*, 102157.

Maitner, Brian S, Brad Boyle, Nathan Casler, Rick Condit, John Donoghue, Sandra M Durán, Daniel Guaderrama, Cody E Hinchliff, Peter M Jørgensen, Nathan JB Kraft et al., "The bien r package: A tool to access the Botanical Information and Ecology Network (BIEN) database," *Methods in Ecology and Evolution*, 2018, *9* (2), 373–379.

Rennert, Kevin, Frank Errickson, Brian C Prest, Lisa Rennels, Richard G Newell, William Pizer, Cora Kingdon, Jordan Wingenroth, Roger Cooke, Bryan Parthum et al., "Comprehensive evidence implies a higher social cost of CO2," *Nature*, 2022, *610* (7933), 687–692.

Saatchi, Sassan S, Nancy L Harris, Sandra Brown, Michael Lefsky, Edward TA Mitchard, William Salas, Brian R Zutta, Wolfgang Buermann, Simon L Lewis, Stephen Hagen et al., "Benchmark map of forest carbon stocks in tropical regions across three continents," *Proceedings of the national academy of sciences*, 2011, *108* (24), 9899–9904.

State Council Information Office of the People's Republic of China, "China's Foreign Aid," 2014. White paper "China's Foreign Aid (2014)".

_ , "China's International Development Cooperation in the New Era," White paper 2021. State Council Information Office, People's Republic of China.

Sun, Liyang and Sarah Abraham, "Estimating dynamic treatment effects in event studies with heterogeneous treatment effects," *Journal of econometrics*, 2021, *225* (2), 175–199.

U.S. Environmental Protection Agency, "Social Cost of Greenhouse Gases: Estimates Incorporating Recent Scientific Advances," Technical Report, U.S. Environmental Protection Agency, Washington, D.C. 2023.

World Bank, *Belt and Road Economics: Opportunities and Risks of Transport Corridors*, Washington, DC: World Bank, 2019.

World Health Organization, "Ambient Air Pollution: A Global Assessment of Exposure and Burden of Disease," 2016.

_ , "WHO Global Air Quality Guidelines: Particulate Matter ($PM_{2.5}$ and PM_{10}), Ozone, Nitrogen Dioxide, Sulfur Dioxide and Carbon Monoxide," 2021.

Xu, Jinqiang, Xuemei Liu, and Churen Sun, "Foreign Aid and Recipient Countries' Participation in Global Value Chains: A Comparative Study Based on Chinese and US Aid: Jinqiang Xu," *Open Economies Review*, 2025, *36* (3), 947–979.

Xu, Zhicheng, Yu Zhang, and Dongying Li, "Chinese aid and nutrition improvement in Sub-Saharan Africa," *Applied Economics*, 2024, *56* (26), 3098–3116.

Figure 1: Overview of Chinese aid projects

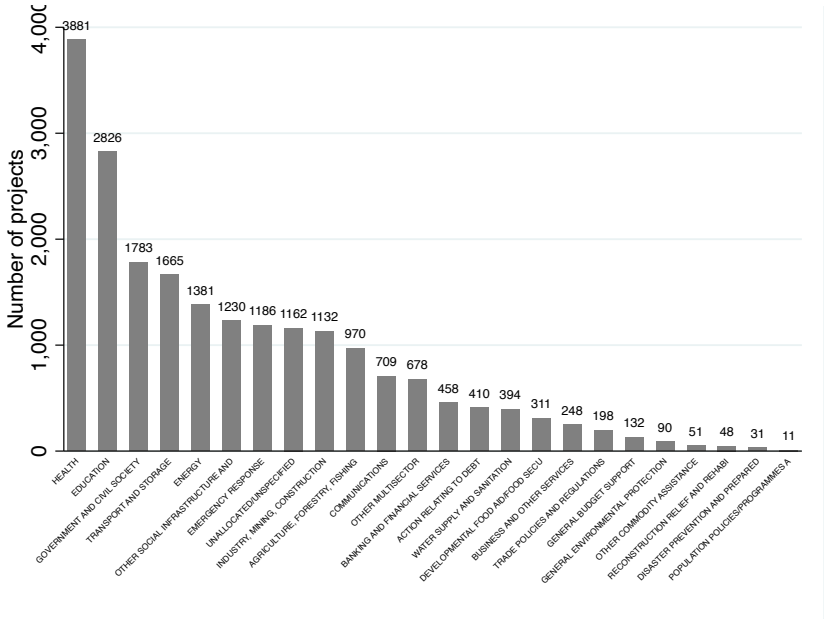

(a) Panel A: Sector composition

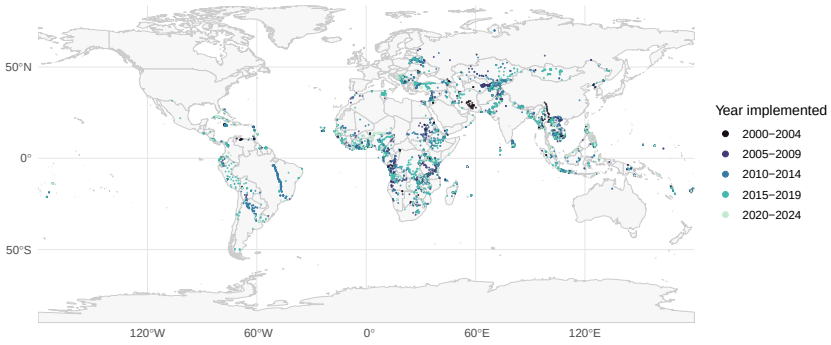

(b) Panel B: Geographic distribution

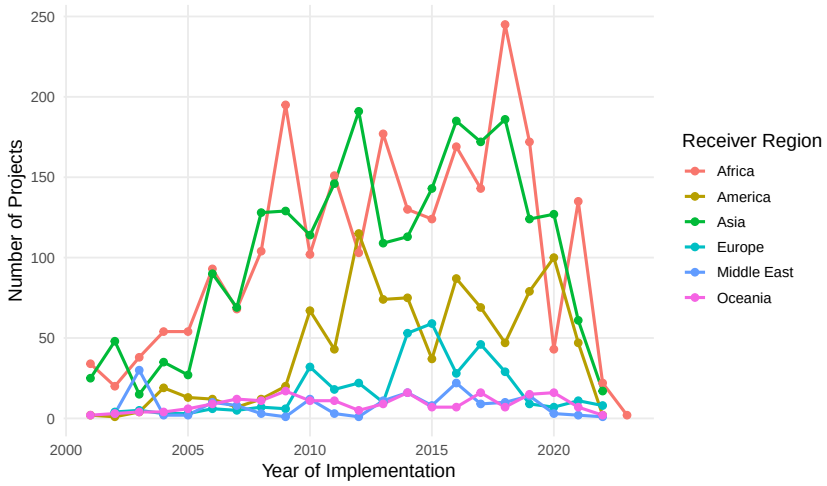

(c) Panel C: Time series of implementation

Figure 2: Event study estimates for NDVI around project implementation

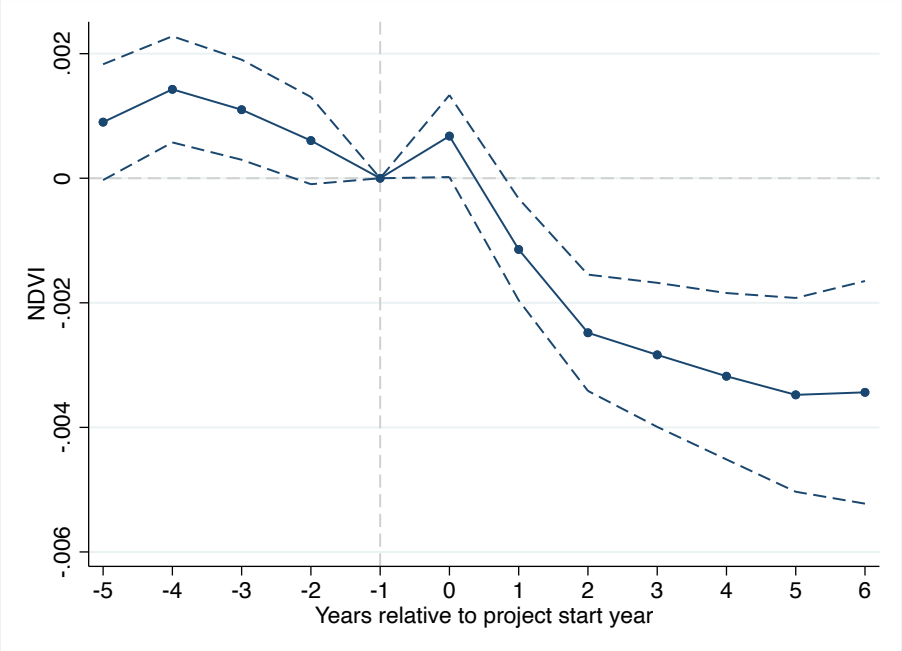

Notes: The figure reports event study coefficients from equation (2), where the omitted category is the period immediately before project implementation. Points represent point estimates and vertical bars indicate 95% confidence intervals based on standard errors clustered at the project-ADM2 level. The sample covers all projects with non-missing implementation dates between 2001 and 2023. Year-month fixed effects and project-ADM2 fixed effects are included in all specifications.

Figure 3: Event study estimates for MERRA-2 AOD around project implementation

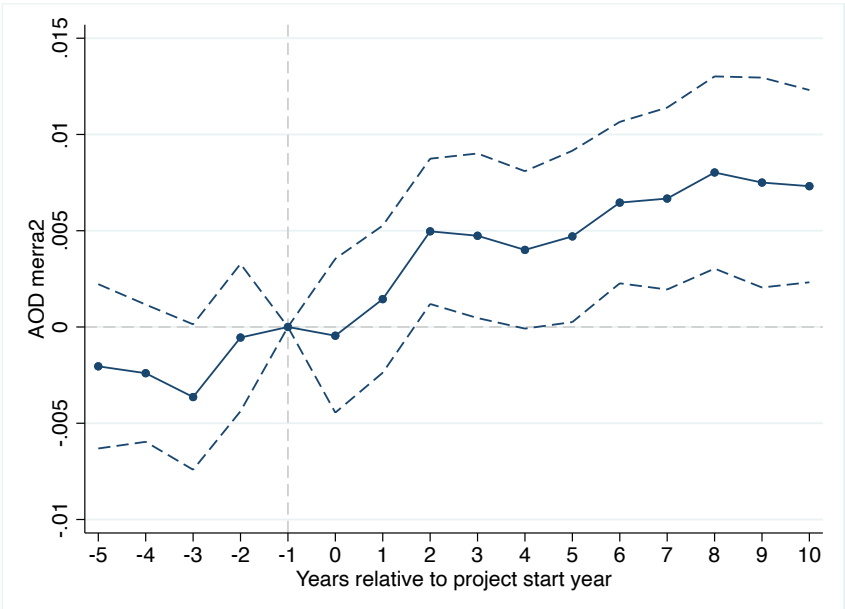

Notes: The figure reports event study coefficients from equation (2), where the omitted category is the period immediately before project implementation. Points represent point estimates and vertical bars indicate 95% confidence intervals based on standard errors clustered at the project-ADM2 level. The dependent variable is monthly aerosol optical depth measured using the MERRA-2 reanalysis product. The sample includes all projects with non-missing implementation dates between 2001 and 2023. All specifications include project-ADM2 fixed effects and year-month fixed effects.

Table 1: Effects of project implementation on NDVI

	NDVI		
Post	-0.00165***	-0.00165***	-0.00114***
	(0.00041)	(0.00041)	(0.00030)
Observations	1738344	1738344	1738344
R-square	0.850	0.850	0.856
Y-mean	0.388	0.388	0.388
Y-sd	0.237	0.237	0.237
Project FEs	Y		
ADM2 FEs	Y		
Project-ADM2 FEs		Y	Y
Year-month FEs	Y	Y	Y
Country-specific trends			Y

Notes: This table reports two-way fixed effects estimates from equation (1). The dependent variable is monthly NDVI measured at the project-ADM2 level. The treatment indicator equals one for all periods after project implementation. Column (1) includes project and ADM2 fixed effects, column (2) replaces these with project-ADM2 fixed effects, and column (3) additionally controls for country-specific linear time trends. All specifications include year-month fixed effects. The sample consists of a balanced panel of project-ADM2 units observed from 2001 to 2023. Standard errors are clustered at the project-ADM2 level.

Table 2: Effects of project implementation on MERRA-2 AOD

	MERRA-2 AOD		
Post	0.00237***	0.00237***	0.00202***
	(0.00036)	(0.00036)	(0.00034)
Observations	1739628	1739628	1739628
R-square	0.472	0.472	0.475
Y-mean	0.233	0.233	0.233
Y-sd	0.167	0.167	0.167
Project FEs	Y		
ADM2 FEs	Y		
Project-ADM2 FEs		Y	Y
Year-month FEs	Y	Y	Y
Country-specific trends			Y

Notes: This table reports two-way fixed effects estimates of the impact of project implementation on aerosol optical depth measured using the MERRA-2 reanalysis product. The dependent variable is monthly AOD aggregated to the project-ADM2 level. Treatment is defined as an indicator equal to one for all months following project implementation. All specifications follow equation (1) and include the fixed effects indicated in each column. The sample covers 2001-2023 and is balanced at the project-ADM2-year-month level. Standard errors are clustered at the project-ADM2 level. Across specifications, project implementation increases MERRA-2 AOD by 0.002 units, corresponding to 0.87% of the sample mean and 1.21% of one standard deviation.

Online Appendix

A Appendix figures

Figure S1: Landsat image near the Batang Toru Hydropower Project

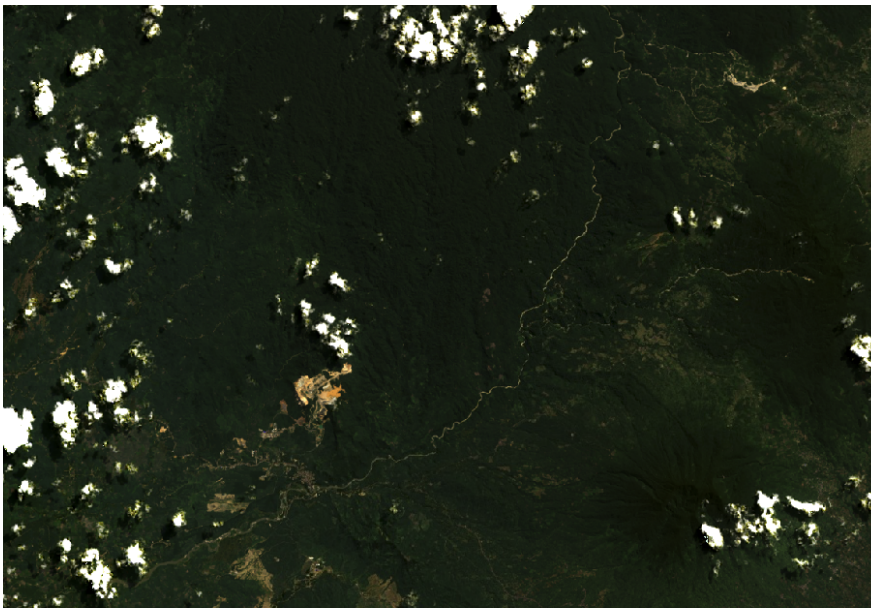

(a) 2013-2014 (pre-construction)

(b) 2023-2024 (post-construction)

Notes: Images are derived from Landsat 8 Surface Reflectance data. The project coordinates are 1.5804°N, 99.1688°E. A cloud cover filter was applied to include only images with less than 20% cloud cover.

Figure S2: Biodiversity near Chinese aid projects

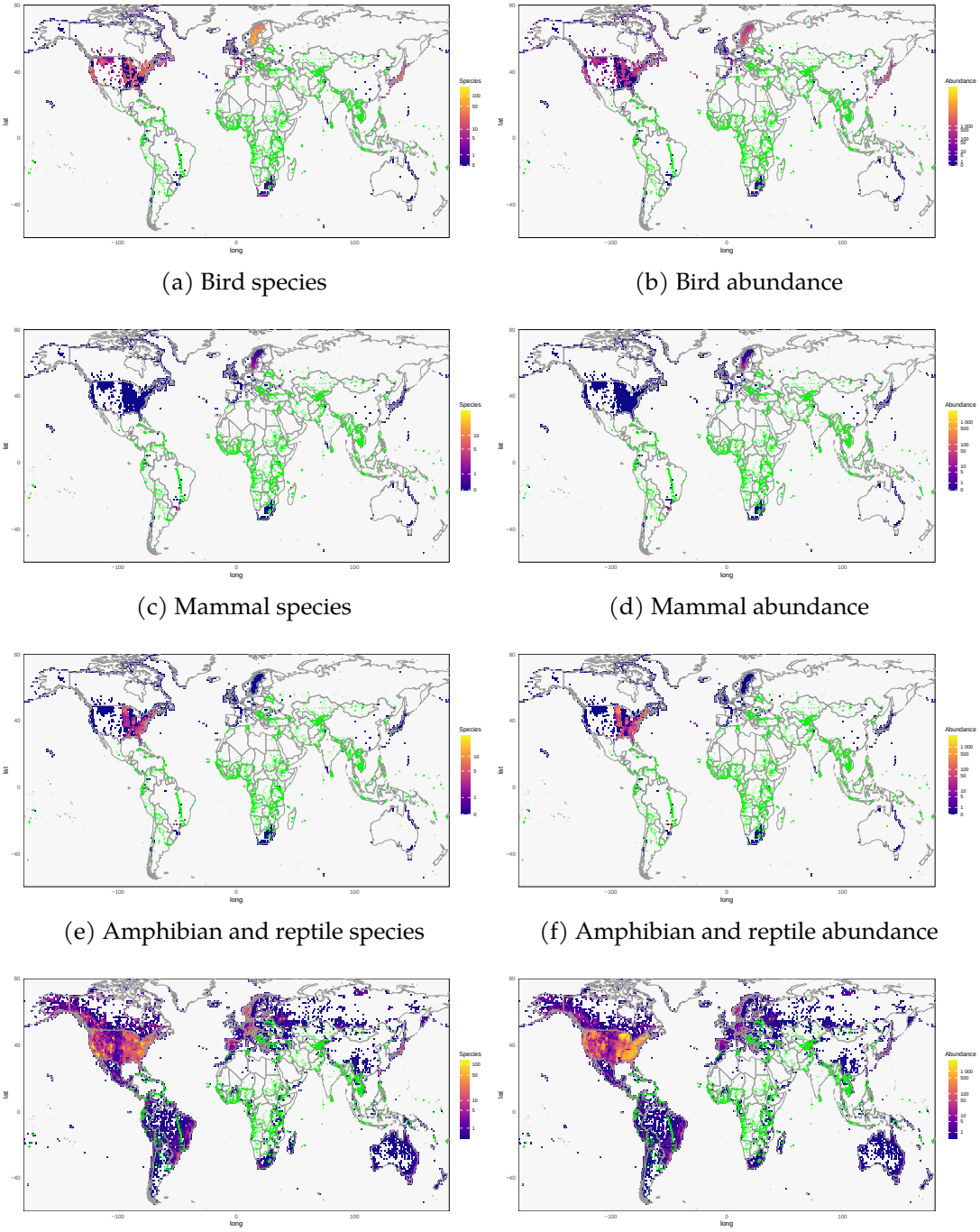

(a) Bird species

(b) Bird abundance

(c) Mammal species

(d) Mammal abundance

(e) Amphibian and reptile species

(f) Amphibian and reptile abundance

(g) Plant species

(h) Plant abundance

Notes: This figure shows the spatial distribution of biodiversity outcomes near Chinese aid project locations. Species richness and abundance are aggregated to the one-degree grid level by taxonomic group and year. Observations are derived from BioTIME and BIEN databases. The map presents large spatial heterogeneity in biodiversity patterns, with higher richness and abundance concentrated in tropical and forested regions where Chinese aid projects are heavily clustered.

Figure S3: Heterogeneity in NDVI effects by project sector

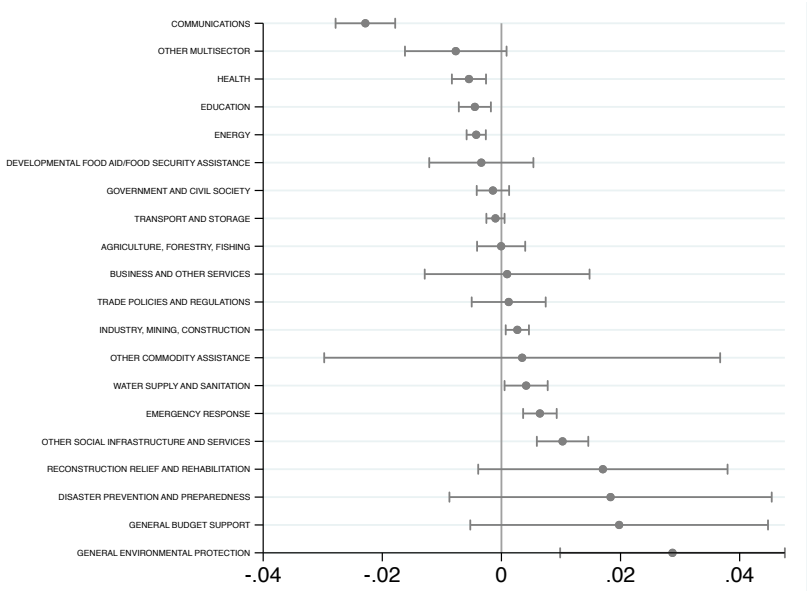

Notes: This figure reports heterogeneous treatment effects of project implementation on NDVI by project sector. Each point represents the estimated post-implementation effect relative to the omitted sector, based on a two-way fixed effects specification with project-ADM2 and year-month fixed effects. Vertical bars indicate 95% confidence intervals constructed from standard errors clustered at the project-ADM2 level.

Figure S4: Heterogeneity in NDVI effects by implementation year

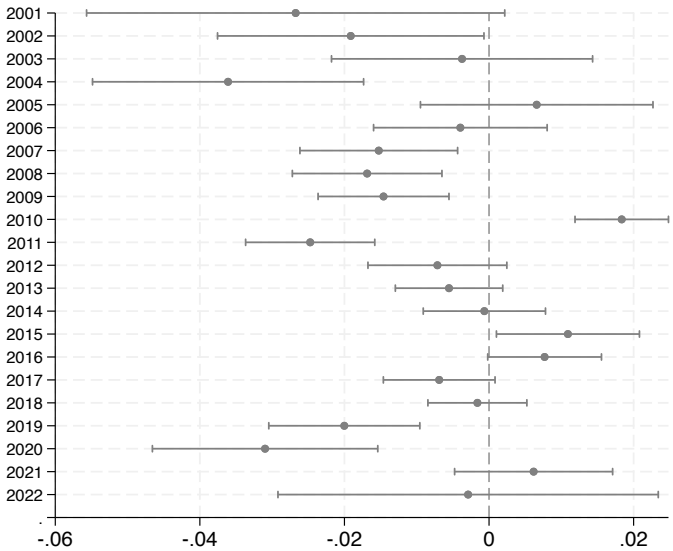

Notes: This figure shows estimated treatment effects on NDVI by project implementation year. Each coefficient is obtained from a two-way fixed effects regression with project-ADM2 and year-month fixed effects. Error bars represent 95% confidence intervals based on standard errors clustered at the project-ADM2 level. Variation across years reflects differences in project composition and geographic exposure rather than global vegetation trends.

Figure S5: Event study estimates for vegetation share around project implementation

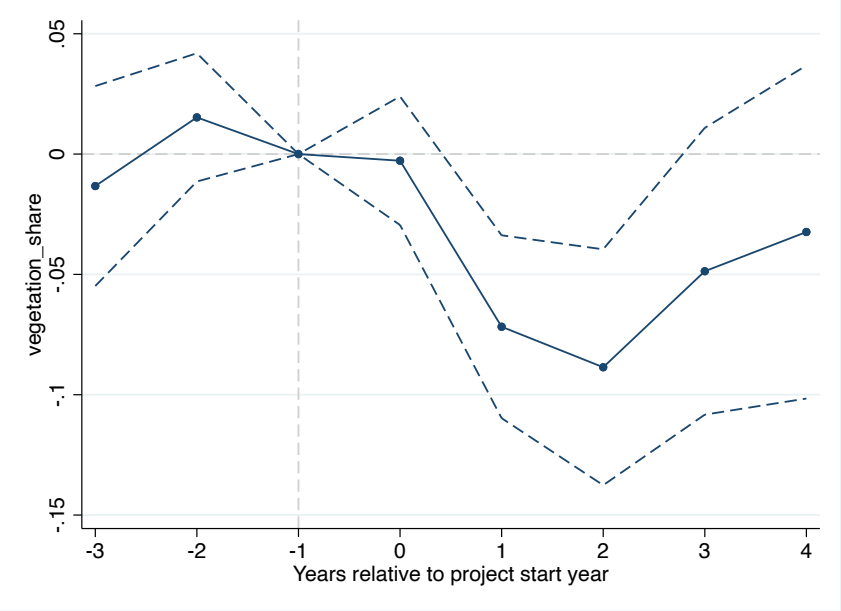

Notes: The figure reports event study coefficients from equation (2), where the omitted category is the period immediately before project implementation. Points represent point estimates and vertical bars indicate 95% confidence intervals based on standard errors clustered at the project-ADM2 level. The dependent variable is total vegetation share, defined as the combined area of forest, woody savanna, savanna, shrubland, and grassland using MODIS land cover classifications. The sample includes all projects with non-missing implementation dates observed between 2001 and 2023. All specifications include project-ADM2 fixed effects and year fixed effects.

Figure S6: Event study estimates for MODIS AOD around project implementation

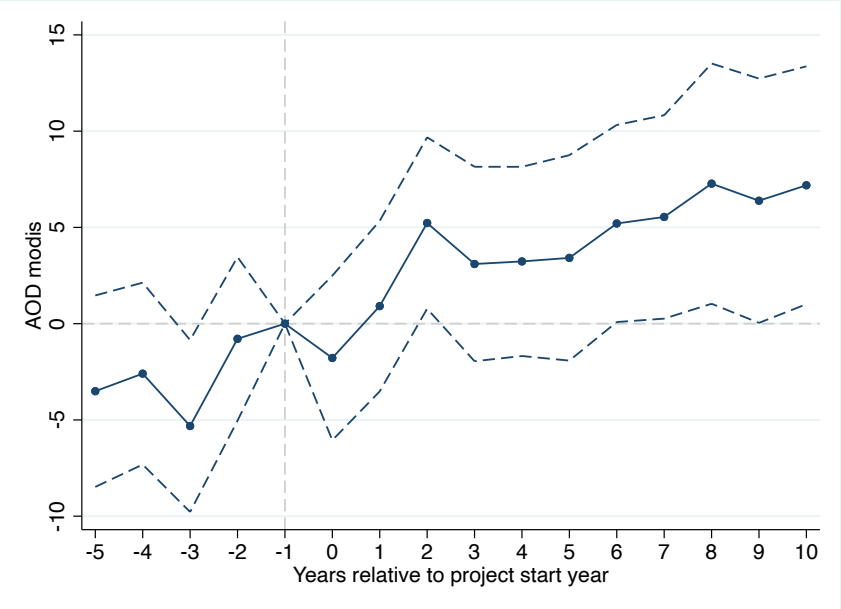

Notes: This figure plots event study coefficients from equation (2), showing the dynamic response of MODIS AOD around project implementation. The omitted period is the year immediately prior to implementation. The vertical dashed line indicates the implementation year. Error bands represent 95% confidence intervals based on standard errors clustered at the project-ADM2 level.

Figure S7: Event study figures using Callaway and Sant'Anna (2021) and Sun and Abraham (2021) estimators

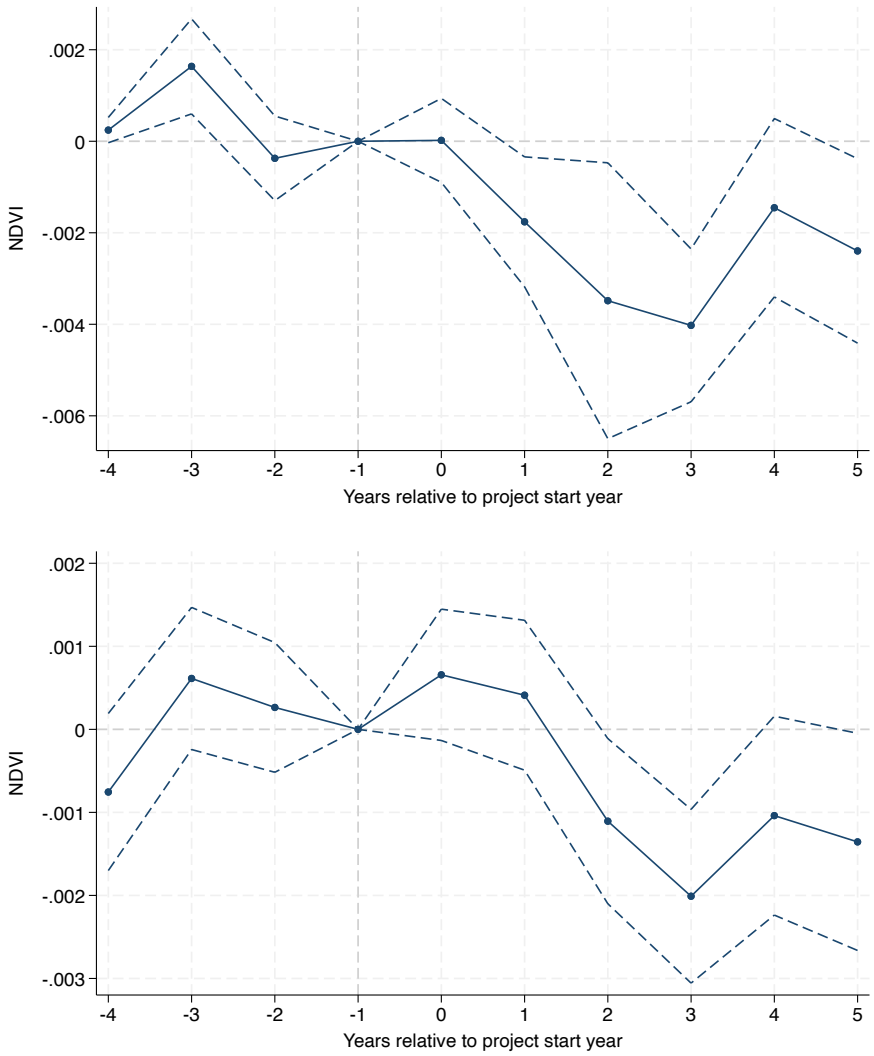

Notes: The figure reports event study coefficients, where the omitted category is the period immediately before project implementation. Points represent point estimates and vertical bars indicate 95% confidence intervals based on standard errors clustered at the project-ADM2 level. The sample is at the project-year level and covers all projects with non-missing implementation dates between 2001 and 2023. Year fixed effects and project-ADM2 fixed effects are included in all specifications.

B Appendix tables

Table S1: Robustness of NDVI effects to alternative treatment definitions

	NDVI	
Post × Amount	-0.00001***	
	(0.00000)	
Post		-0.00231***
		(0.00060)
Observations	1738344	1738344
R-square	0.850	0.850
Y-mean	0.388	0.388
Y-sd	0.237	0.237
Project-ADM2 FEs	Y	Y
Year-month FEs	Y	Y

Notes: This table assesses the robustness of estimated NDVI effects to alternative definitions of treatment. Column (1) redefines treatment timing using project completion dates instead of implementation dates to account for potential lags between administrative approval and on-the-ground activity. Column (2) weights treatment intensity by project investment amount to capture variation in construction scale. All specifications follow the baseline two-way fixed effects model with project-ADM2 and year-month fixed effects. The sample is a balanced project-ADM2-year-month panel from 2001 to 2023. Standard errors are clustered at the project-ADM2 level.

Table S2: Heterogeneity in NDVI effects by country income group

	Low income	Lower middle income	Upper middle income
Post	-0.00196***	0.00002	-0.00110
	(0.00039)	(0.00075)	(0.00125)
Observations	878508	400355	426233
R-square	0.823	0.872	0.864
Y-mean	0.433	0.365	0.332
Y-sd	0.216	0.230	0.251
Project-ADM2 FEs	Y	Y	Y
Year-month FEs	Y	Y	Y

Notes: This table reports heterogeneous effects of project implementation on NDVI across World Bank income groups of recipient countries. Separate regressions are estimated for each group using the baseline two-way fixed effects specification. All models include project-ADM2 fixed effects and year-month fixed effects, and are estimated on a balanced project-ADM2-year-month panel from 2001 to 2023. Standard errors are clustered at the project-ADM2 level. The estimates indicate that vegetation loss following project implementation is more pronounced in lower-income settings, consistent with weaker environmental regulation and lower enforcement capacity during construction activity.

Table S3: Heterogeneity in NDVI effects by region

	Africa	Asia	America	Europe	Oceania	Middle East
Post	-0.00239***	-0.00149***	-0.00304*	0.00424***	0.00094	0.00349
	(0.00054)	(0.00039)	(0.00177)	(0.00129)	(0.00217)	(0.00217)
Observations	656328	621244	257232	101972	54372	47196
R-square	0.816	0.887	0.903	0.819	0.928	0.727
Y-mean	0.405	0.408	0.352	0.468	0.206	0.122
Y-sd	0.233	0.214	0.274	0.176	0.271	0.089
Project-ADM2 FEs	Y	Y	Y	Y	Y	Y
Year-month FEs	Y	Y	Y	Y	Y	Y

Notes: This table reports heterogeneous effects of project implementation on NDVI across world regions. Separate regressions are estimated for each region using the baseline two-way fixed effects specification. All models include project-ADM2 fixed effects and year-month fixed effects and are estimated on a balanced project-ADM2-year-month panel from 2001 to 2023. Standard errors are clustered at the project-ADM2 level. The estimates reveal stronger vegetation declines in Africa, Asia, and the Americas, where Chinese overseas construction is more concentrated and often intersects with ecologically sensitive landscapes, while effects are smaller and less precise in Europe, Oceania, and the Middle East.

Table S4: Heterogeneity in NDVI effects by project intent

	Development	Commercial	Mixed	Representational
Post	0.00047	0.00166	-0.00324***	-0.00285
	(0.00054)	(0.00240)	(0.00072)	(0.00566)
Observations	1042549	44722	638976	12097
R-square	0.855	0.840	0.838	0.819
Y-mean	0.371	0.327	0.421	0.381
Y-sd	0.245	0.229	0.220	0.217
Project-ADM2 FEs	Y	Y	Y	Y
Year-month FEs	Y	Y	Y	Y

Notes: This table reports heterogeneous effects of project implementation on NDVI by project intent category. Separate regressions are estimated for development, commercial, mixed, and representational projects using the baseline two-way fixed effects specification. All specifications include project-ADM2 fixed effects and year-month fixed effects and are estimated on a balanced project-ADM2-year-month panel from 2001 to 2023. Standard errors are clustered at the project-ADM2 level. The results indicate that vegetation declines are largest for mixed and representational projects, which typically involve larger physical footprints or more intensive site development, while development and commercially oriented projects exhibit comparatively smaller NDVI reductions.

Table S5: Heterogeneity in NDVI effects by funder

	Panel A: Funder type					
	Government agency	Policy bank	Commercial bank	State-owned company	State-owned fund	Mixed
Post	-0.00007	-0.00335***	0.00309***	0.00895***	0.00363	-0.00685*
	(0.00063)	(0.00066)	(0.00112)	(0.00293)	(0.00487)	(0.00407)
Observations	730786	775815	144506	61941	2400	22896
R-square	0.860	0.832	0.839	0.828	0.694	0.890
Y-mean	0.349	0.434	0.370	0.341	0.348	0.339
Y-sd	0.251	0.222	0.206	0.215	0.161	0.221
	Panel B: Specific funder					
	CDB	Eximbank	Ministry of Commerce	Chinese Embassy		
Post	-0.00179*	-0.00451***	-0.00000	-0.00420		
	(0.00106)	(0.00074)	(0.00091)	(0.00262)		
Observations	165835	622388	305532	65688		
R-square	0.000	0.837	0.870	0.837		
Y-mean	0.459	0.425	0.348	0.338		
Y-sd	0.214	0.224	0.268	0.248		
Project-ADM2 FEs	Y	Y	Y	Y	Y	Y
Year-month FEs	Y	Y	Y	Y	Y	Y

Notes: This table reports heterogeneous effects of project implementation on NDVI by funder. In Panel A, we focus on funder type, and separate regressions are estimated for projects financed by government agencies, policy banks, commercial banks, state-owned companies, state-owned funds, and projects with mixed funding sources, using the baseline two-way fixed effects specification. Panel B focuses on the top four specific funders: the two policy banks, China Development Bank (CDB) and Export-Import Bank (Eximbank), and two government agencies, the Ministry of Commerce and the Chinese Embassy. All models include project-ADM2 fixed effects and year-month fixed effects and are estimated on a balanced project-ADM2-year-month panel covering 2001 to 2023. Standard errors are clustered at the project-ADM2 level.

Table S6: Heterogeneity in NDVI effects by baseline NDVI quartile

	1st quartile	2nd quartile	3rd quartile	4th quartile
Post	-0.00067	-0.00132**	-0.00218***	-0.00184***
	(0.00111)	(0.00067)	(0.00060)	(0.00037)
Observations	434000	434120	434696	434424
R-square	0.724	0.291	0.182	0.380
Y-mean	0.092	0.329	0.491	0.639
Y-sd	0.154	0.111	0.112	0.104
Project-ADM2 FEs	Y	Y	Y	Y
Year-month FEs	Y	Y	Y	Y

Notes: This table reports heterogeneous effects of project implementation on NDVI by baseline NDVI quartile, where quartiles are defined using the pre-implementation distribution of NDVI at the project-ADM2 level. Separate regressions are estimated for each quartile using the baseline two-way fixed effects specification. All models include project-ADM2 fixed effects and year-month fixed effects and are estimated on a balanced project-ADM2-year-month panel covering 2001 to 2023. Standard errors are clustered at the project-ADM2 level.

Table S7: Effects of project implementation on land cover

	Forest share		
Post	0.07248	0.07248	0.00298
	(0.04667)	(0.04583)	(0.04032)
Observations	144969	144969	144969
R-square	0.985	0.985	0.990
Y-mean	12.132	12.132	12.132
Y-sd	19.692	19.692	19.692
Project FEs	Y		
ADM2 FEs	Y		
Project-ADM2 FEs		Y	Y
Year FEs	Y	Y	Y
Country-specific trends			Y
	Broadtree share		
Post	0.04339	0.04339	0.04289
	(0.03797)	(0.03728)	(0.03414)
Observations	144969	144969	144969
R-square	0.994	0.994	0.995
Y-mean	33.094	33.094	33.094
Y-sd	32.260	32.260	32.260
Project FEs	Y		
ADM2 FEs	Y		
Project-ADM2 FEs		Y	Y
Year FEs	Y	Y	Y
Country-specific trends			Y
	Vegetation share		
Post	-0.11413***	-0.11413***	-0.08966***
	(0.02960)	(0.02906)	(0.02770)
Observations	144969	144969	144969
R-square	0.996	0.996	0.997
Y-mean	58.026	58.026	58.026
Y-sd	32.012	32.012	32.012
Project FEs	Y		
ADM2 FEs	Y		
Project-ADM2 FEs		Y	Y
Year FEs	Y	Y	Y
Country-specific trends			Y

Notes: This table reports two-way fixed effects estimates from equation (1). Outcomes are annual land cover shares measured at the project-ADM2 level using MODIS classifications. Panel A reports effects on forest share. Panel B expands the outcome to include woody savanna and savanna (broadtree share). Panel C reports effects on total vegetation share, defined as the combined area of forest, woody savanna, savanna, shrubland, and grassland. The treatment indicator equals one for all years following project implementation. Column (1) includes project and ADM2 fixed effects, column (2) replaces these with project-ADM2 fixed effects, and column (3) additionally controls for country-specific linear time trends. All specifications include year fixed effects. The sample consists of a balanced panel of project-ADM2 units observed from 2001 to 2023. Standard errors are clustered at the project-ADM2 level.

Table S8: Effects of project implementation on MODIS AOD

	MODIS AOD		
Post	2.22441***	2.22441***	1.94251***
	(0.47504)	(0.47432)	(0.44315)
Observations	1717376	1717376	1717376
R-square	0.460	0.460	0.463
Y-mean	293.976	293.976	293.976
Y-sd	204.482	204.482	204.482
Project FEs	Y		
ADM2 FEs	Y		
Project-ADM2 FEs		Y	Y
Year-month FEs	Y	Y	Y
Country-specific trends			Y

Notes: This table reports the estimated effects of project implementation on aerosol optical depth measured using MODIS satellite data. The analysis is conducted at the project-ADM2-year-month level using a balanced panel spanning 2001 to 2023. All specifications follow the baseline two-way fixed effects model and progressively add more restrictive fixed effects. Project-ADM2 fixed effects absorb time-invariant local characteristics, while year-month fixed effects control for global temporal shocks and seasonal patterns. The final specification further includes country-specific linear time trends. Standard errors are clustered at the project-ADM2 level.

Table S9: Correlation between vegetation and biodiversity

	Panel A: NDVI and species richness			
	Plants	Birds	Mammals	Amphibians & reptiles
NDVI	0.42336***	5.43634***	6.93845*	-4.68289
	(0.14640)	(1.56268)	(3.49940)	(4.92284)
Observations	16353	483	115	115
R-square	0.411	0.523	0.575	0.198
Y-mean	0.245	0.652	1.005	0.391
Y-sd	0.631	1.261	1.483	1.013
	Panel B: NDVI and abundance			
NDVI	0.35847**	9.85145***	15.36573*	-6.70621
	(0.17719)	(2.99291)	(8.57988)	(8.47035)
Observations	16353	483	115	115
R-square	0.411	0.527	0.519	0.200
Y-mean	0.290	1.199	2.210	0.703
Y-sd	0.764	2.424	3.419	1.746
	Panel C: Vegetation share and species richness			
Vegetation share	0.00476**	-0.00901	-0.06830	-0.19241
	(0.00233)	(0.02889)	(0.23016)	(0.55910)
Observations	16353	483	115	115
R-square	0.410	0.510	0.556	0.191
Y-mean	0.245	0.652	1.005	0.391
Y-sd	0.631	1.261	1.483	1.013
	Panel D: Vegetation share and abundance			
Vegetation share	0.00602**	0.03056	0.66204	-0.17914
	(0.00283)	(0.05524)	(0.55784)	(0.96094)
Observations	16353	483	115	115
R-square	0.411	0.515	0.509	0.194
Y-mean	0.290	1.199	2.210	0.703
Y-sd	0.764	2.424	3.419	1.746

Notes: This table reports correlations between vegetation measures and biodiversity outcomes at the one-degree grid-year level for the period 2001-2023. NDVI is measured using Landsat data and vegetation share is constructed from MODIS land cover classifications. Species richness and abundance are computed from BioTIME and BIEN observations aggregated by taxon and grid. All specifications include grid and year fixed effects. The sample is restricted to grids that contain at least one Chinese aid project and at least one biodiversity observation for the corresponding taxon.

Table S10: Effects of project implementation on biodiversity

	ln(Species count + 1)			
	Plants	Birds	Mammals	Amphibians & reptiles
Post	-0.00255	-0.01562*	-0.00101*	-0.00158**
	(0.00468)	(0.00851)	(0.00061)	(0.00064)
Observations	144969	144969	144969	144969
R-square	0.333	0.205	0.658	0.137
Y-mean	0.068	0.010	0.002	0.000
Y-sd	0.330	0.188	0.076	0.034
	ln(Abundance + 1)			
Post	-0.00206	-0.03101*	-0.00219	-0.00301**
	(0.00550)	(0.01716)	(0.00140)	(0.00123)
Observations	144969	144969	144969	144969
R-square	0.343	0.212	0.643	0.143
Y-mean	0.080	0.020	0.003	0.001
Y-sd	0.398	0.366	0.167	0.068

Notes: This table reports two-way fixed effects estimates of the impact of project implementation on biodiversity outcomes. The unit of observation is the project-grid-year. Treatment is defined as an indicator equal to one for all years following project implementation. Species richness and abundance are measured as ln(outcome + 1). All specifications follow equation (1) and include project-grid and year fixed effects. The panel covers 2001-2023. Standard errors are clustered at the project-grid level.